Interference effects with surface plasmons

Kuzmin, N.V.

Chapter 6

Retardation effects in sub-wavelength slits in thin metal films near cut-off

We have experimentally studied the transmission properties of a single sub-wavelength-wide slit in a 200 nm thick Au film as a function the the slit width, for both TE and TM polarizations. Contrary to the standard waveguide model for an ideal metal that predicts a cut-off for the TE mode at a slit width equal to $b = \lambda/2$, we find that the transmission for TM and TE polarized incident light is approximately equal at $b = \lambda/4$ ($\lambda = 800$ nm), and that the TE transmission becomes negligible only when $b \simeq \lambda/8$. A polarization analysis of the transmitted light shows that at $b = \lambda/4$ the slit acts as a quarter-wave plate. Calculations based on rigorous diffraction theory are in good agreement with the experimental results.

6.1 Introduction

In 1861 Fizeau described in a remarkable paper his observations on the polarization properties of natural light as it was transmitted through a wedge-shaped scratch in a thin silver film [104]. He discovered that the light transmitted through the narrowest sections of the slit is polarized perpendicular to the slit, while the light transmitted through somewhat wider sections is predominantly polarized parallel to the slit. He compared a whole range of metals, such as gold, brass, tin, iron, etc. and found similar results for all these materials. In his paper Fizeau also presents values for the film thickness (of order 200 nm) and the slit width (of order 100 nm). Fizeau did not have a theoretical framework to explain his results because Maxwell's theory of electromagnetism had not yet been developed.

Sub-wavelength slit apertures in metal screens came back into the focus of attention in the context of the development of radar around the time of the second world war. The polarizing action of such apertures could now be explained in terms of electromagnetic theory, using a description in terms of a waveguide consisting of two plane-parallel metallic sheets [105]. In that model the strong polarizing action of the narrowest slits comes about because these slits allow only one polarization mode to propagate with low loss, while the other is extremely lossy, being evanescent. The development of novel astronomical and spectroscopic techniques in subsequent years provided another push to study this subject but now at optical wavelengths, i.e., on a much smaller spatial scale [106–108]. At these wavelengths ohmic damping in the metal can not be ignored.

The issue of the transmission of very small *circular* holes was discussed by Bethe in a landmark paper in 1944 [37], predicting that the transmission of a hole with radius $a \ll \lambda$ scales as $(a/\lambda)^6$. This work was extended by Bouwkamp [109]; the resulting theoretical model is known as the Bethe-Bouwkamp theory and has played an important role in the development of optical recording techniques [110].

Sub-wavelength apertures in thin metallic films were suddenly rocketed to center stage by the recent observation that a regular (two-dimensional) array of such apertures has a much larger transmission than what one expects based on Bethe's theory [36]. In these studies [72] both the hole diameter and the thicknesses of the metal film are of the order of a few hundred nanometers, smaller than the wavelength of the incident light. The transmission spectrum of such a hole array displays sharp resonances; these resonances vanish when the apertures are arranged in an arbitrary pattern. The standard explanation of these phenomena is that the regular array of holes acts as a grating that couples the

incident field to a surface wave; the latter is scattered to a transmitted wave by the same grating-like structure. The transmission spectrum then carries information about the various gratings that are contained in the hole array while the line shape of an individual resonance reflects the interference between the light that is directly transmitted (in a Bethe-like fashion) by the holes and the channel that involves a surface wave as an intermediary [111,112]. It is widely accepted that surface plasmon polaritons, henceforth called surface plasmons, are responsible for this effect although this explanation is contested [51]. In these experiments all relevant dimensions (wavelength of incident radiation, hole diameter, film thickness) have sub-micron, i.e., nanometric size. For that reason, it belongs to the field of nano-optics. Similar results, i.e., pronounced spectral signatures, are also obtained for metallic films featuring a single hole surrounded by equidistant circular grooves or a slit surrounded by parallel equidistant trenches [111].

In the experiments on two-dimensional hole arrays the polarization of the incident radiation plays an important role in that it determines the surface-plasmon modes (Bloch waves) that the incident beam can couple to. In a 1D structure, such as a parallel slit array (grating) or a slit surrounded by parallel, equidistant grooves, the polarization of the incident light has a much more pronounced effect. Only when the latter has a component perpendicular to the slits (so-called TM-polarization) does the incident light couple to surface plasmons. When the light is polarized parallel to the slits these surface modes do not come into play. Most of this was known already from the study of the the diffraction properties of metallic gratings [113].

Recent theoretical and experimental work on the transmission of single slits has focussed on slits that have a sub-wavelength width [41, 43, 48, 114]. For TM-polarized incident light these authors predict or observe Fabry-Pérot resonances when the thickness of the metallic screen exceeds $\lambda/(2n_z)$ where n_z is the index of refraction of the metallic waveguide for the TM-polarized mode. The TE-polarized mode has received much less attention and, seemingly, for a good reason. Universally accepted waveguide models predict that a narrow slit does not transmit such a mode when its wavelength is beyond cut-off. For perfect metals the cut-off wavelength equals twice the slit width; for real metals the cut-off wavelength is somewhat larger [56, 115]. All these models predict a rather pronounced resonance in the transmission spectrum of a single slit at a wavelength just before cut-off [116–122].

Our interest in this field was triggered by a series of measurements on sub-wavelength double slits [61]. In these experiments we showed that surface plasmons act to modulate the *spectrum* of such a double slit. In order to argue

that the spectral modulation is indeed due to surface plasmons we used TM-polarized incident light, allowing excitation of these surface modes, and TE-polarized incident light, where surface plasmons can not be excited. It came as a surprise when we measured that the transmittivity of the slits (200 nm wide in a 200 nm thick gold metal film) for incident light at a wavelength of $\simeq 800$ nm was *of the same order of magnitude for both input polarizations*. In view of the fact that the slits were much narrower than the wavelength of the incident radiation ($b/\lambda \simeq 0.25$) the TE-transmission was, naively, expected to be orders of magnitude smaller than that for the TM-polarization. A rigorous theoretical scattering model based on a Green's function approach predicted that the TE-polarized transmission is not negligible but, typically, an order of magnitude smaller than that for the TM polarization [61]. Experiments using similar samples prepared under slightly different conditions confirmed our initial experimental results. Clearly, they could not be attributed to a single anomalous sample.

In a subsequent study we investigated the polarization properties of the double slit or, more accurately, each of the pair of slits. The questions we wanted to address are: i) what is the polarization state of the transmitted light when the polarization of the incident light is purely TE or TM; ii) what is the polarization state of the transmitted light when the incident light is circularly polarized? The results are shown in Fig. 6.1: when the incident light is either TM- or TE-polarized the transmitted light is fully polarized and has the same polarization as the incident light. However, when the incident light is *circularly* polarized the transmitted light is *linearly* polarized at an angle of 45° relative to the TM- and TE-directions in a way similar to a quarter-wave plate. To complete our measurements we also measured the polarization of the transmitted light for incident light polarized at an angle of 45° relative to the TM- and TE-axes, and found it to be circular. The last two observations imply that the attenuation of the TE and TM-polarized components are approximately equal, and that the propagation constants of the TE- and TM-polarized modes in the slits must be quite different to induce a phase slip of $\pi/2$ over a length of just 200 nm. Effectively, we find $|n_{\mathrm{TE}} - n_{\mathrm{TM}}| = 1$. It appears that such a sub-wavelength slit acts as a lossy, non-dichroic, birefringent optical element.

Here we present a systematic study of the polarization properties of the light transmitted by a single sub-wavelength slit of variable width (50–500 nm) milled in a 200 nm thick gold metal film using incident light at a wavelength of $\simeq 800$ nm. We confirm our first observations and explore at what slit widths the TE-mode is really beyond cut-off. We compare our results with numerical

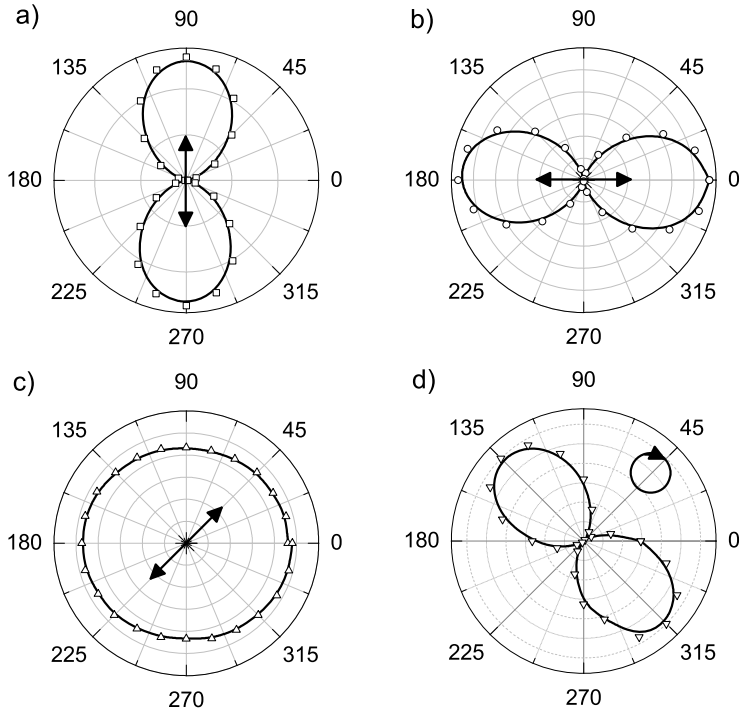

Figure 6.1. Polar plots of the transmission of a single sub-wavelength slit in a thin gold film as a function of the orientation of an analyzing polarisator. The results apply to a 200 nm wide slit milled in a 200 nm thick gold film for incident light at a wavelength of 800 nm. In a) the incident light is TM polarized (perpendicular to the slit axis); in b) it is TE polarized (parallel to the slit axis); in c) it is polarized at an angle of 45° ; in d) it is circularly polarized.

calculations based on rigorous diffraction theory.

6.2 Experiment

In the experiment we analyze the light intensity, transmitted through a 1×10 array of 10 μm long and 50–500 nm wide slits, milled in a 200 nm thick gold film. The width of the slits increases stepwise from 50 nm, well below the cut-off width for TE polarized light at $\lambda = 800$ nm, to 500 nm, at which value the lowest TE-mode can propagate through the slit. The film is deposited on a 0.5 mm thick D263T borosilicate glass substrate, covered by a 10 nm titanium

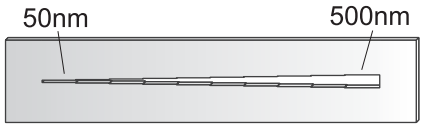

Figure 6.2. Array of sub-wavelength slits.

adhesion layer.

The slits are arranged in a single line (see Fig. 6.2) to simplify the data acquisition: we illuminate all slits in one shot with the beam of a wavelength-tunable ($\lambda \approx 800$ nm). The laser beam has a diameter of ≈ 2 mm at the sample so that the intensity varies only weakly across the composite slit and the laser beam's phase front is approximately flat. An important argument to set the sub-slits along the single line, rather than arranging them in a grating-like way, is that when the surface plasmons are excited by any slit they are not "received" by any other slit.

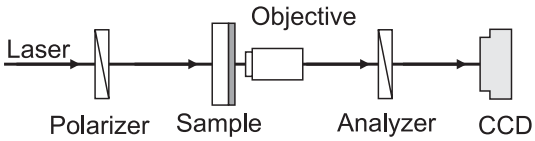

Figure 6.3. Experimental setup. The sample is illuminated from the glass side; the transmitted light is polarization analyzed and imaged on a CCD camera.

The light transmitted by structure is imaged on a CCD camera (Apogee, Alta U1) by means of a 0.65 N.A. microscope objective (Fig. 6.3). The polarization of the light incident on the structure was set to being parallel to the slits (TE polarization), perpendicular to the slits (TM polarization) or at 45° to the slits, containing both TM and TE components.

6.3 Experimental results

We have performed two types of experiments with the array of slits: i) we have measured the total power transmission of all individual slits for the case that the incident light is purely TE- or TM-polarized and ii) we have measured the transmission as a function of the angle of the analyzing polarizer for the case that the incident light is polarized at an angle of 45° relative to the long axis of the slit. The latter measurements provide information on the difference in propagation phase of the TM- and TE-polarized components of the light as it

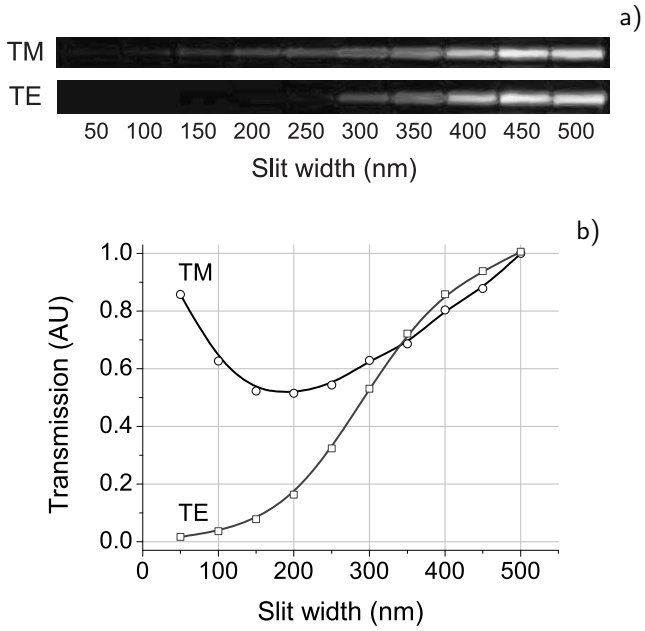

Figure 6.4. a) Slit images for TM or TE illumination; b) Normalized transmittivities ($\lambda = 800$ nm) of TM- or TE-polarized incident light as a function of the slit width. At a slit width of 500 nm the transmission for TE- and TM-polarized incident light at $\lambda = 800$ nm is almost exactly equal. We have, arbitrarily, set the transmission to 1 at this value of the slit width.

propagates through a slit.

6.3.1 Transmission of purely TE/TM polarized incident light.

The recorded images of the slit array for the case that the incident light is either purely TE- or TM- polarized are shown in Fig. 6.4a. It is seen that the TM mode transmits down to the smallest slit width (50 nm) whereas the TE mode essentially becomes opaque when the slit width $b < 250$ nm.

In order to get meaningful results we normalize the signal integrated over the slit, by the slit width. Figure 6.4b shows the normalized transmission data as the function of the slit width. Henceforth, we will discuss the normalized slit transmittivity.

As the slit width is reduced the slit transmission decreases by roughly the same factor for the TE and TM polarizations until $b \simeq 350$ nm. When b is further reduced the normalized TM transmission goes through a minimum at

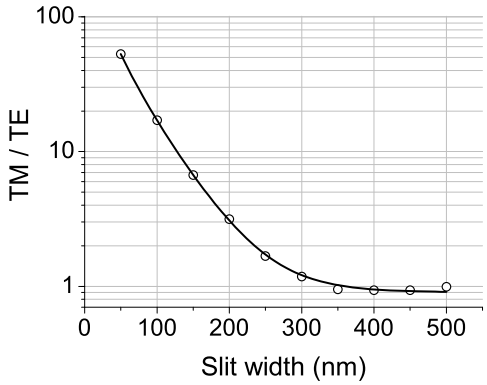

Figure 6.5. TM/TE transmission ratio at $\lambda = 800$ nm of a single sub-wavelength slit, milled in 200 nm thick Au film, as a function of the slit width.

$b \simeq 200$ nm to increase again when b gets even smaller. When we plot the non-normalized transmission power as a function of the slit width we find that power depends linearly on the slit width. Figure 6.4 shows that the normalized TE transmission, however, decreases monotonously. At $b = 50$ nm the TE-transmission is only ~ 2 % of that for the TM polarization. From the data of Figure 6.4b we extract the TM/TE transmission ratio which we plot in Fig. 6.5. Apparently, a narrow slit in a thin metal film is not such a good polarizer as often assumed.

6.3.2 Polarization analysis of transmitted light

To gain a better understanding of the physics associated with the data of Fig. 6.1 we have made a systematic study of the polarization properties of the light transmitted by a sub-wavelength slit as a function of the slit width. We use the array of Fig. 6.2 with normally incident light at $\lambda_{\text{inc}} = 800$ nm, polarized at an angle of 45° relative to the slit. The transmitted light is sent through an analyzing polarizer and is detected as a function of the orientation of this analyzer. The results are shown in Fig. 6.6, in a series of polar plots. As the slit width is reduced from 500 nm to 300 nm the transmitted light gradually becomes more and more elliptically polarized (the minimum transmission increases gradually), while the main axis of the polarization ellipse remains oriented along the polarization direction of the incident light, namely at 45° to the slit. As the slit width is reduced further, the transmitted light becomes more and more linearly polarized, ultimately being purely TM-polarized at

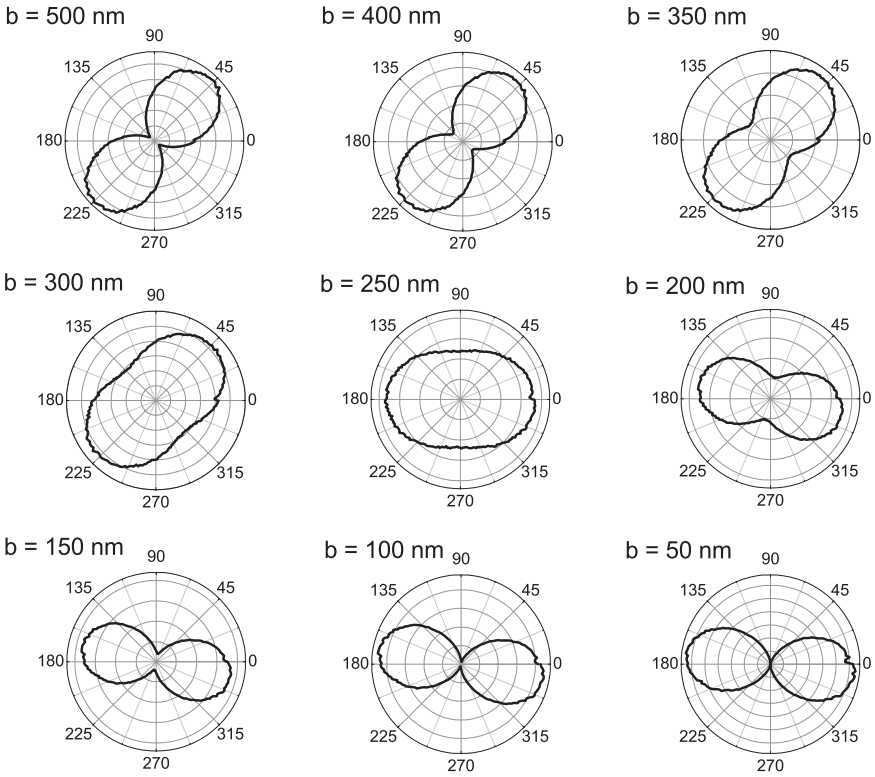

Figure 6.6. Polar diagrams of the measured signal as a function of the orientation of the analyzing polarisator.

$b = 50$ nm.

The directions parallel and perpendicular to the slit are its eigenpolarizations, each with its own damping and propagation constant. In a general case such a slit is therefore both dichroic and birefringent, both properties depending on the ratio b/λ. The effect that we observe as the slit width is decreased from 500 to 300 nm can be explained in terms of an increasing birefringence and negligible dichroism. At $b = 250$ nm, the main axis of the polarization ellipse is rotated, pointing in a direction that is almost perpendicular to the slit. This sudden change is due to the fact that, at $b = 250$ nm, dichroism has become important, as already evident from Fig. 6.5. If the slit width is further decreased, the dichroic effect becomes even larger (see Fig. 6.5). The TE-polarized component of the transmitted light becomes weaker and weaker causing the polar diagram to collapse to a $\cos^2$ pattern. Note that in the

present experiment we do not generate purely circularly polarized light as in the experiment of Fig. 6.1. We attribute this to the use of a different sample with slightly different properties.

In order to extract the phase lag $\Delta\phi$ between the TE- and TM-polarized components of the transmitted field we write the incident field as:

$$\mathbf{E}_{\text{in}} = \begin{pmatrix} E_{\text{TM}} \\ E_{\text{TE}} \end{pmatrix} = \begin{pmatrix} 1 \\ 1 \end{pmatrix}. \tag{6.1}$$

The amplitude-transmission through the slit can be represented by the matrix:

$$\mathbf{T} = \begin{pmatrix} t_{\text{TM}}\, \mathrm{e}^{i\Delta\phi} & 0 \\ 0 & t_{\text{TE}} \end{pmatrix}, \tag{6.2}$$

while the action of the analyzing polarizer, oriented at an angle ψ, is given by:

$$\mathbf{P} = \begin{pmatrix} \cos\psi \\ \sin\psi \end{pmatrix}. \tag{6.3}$$

The amplitude of the transmitted field can be written as:

$$|E_{\text{out}}| = \mathbf{P}^T\, \mathbf{T}\, \mathbf{E}_{\text{in}} = t_{\text{TM}}\, \mathrm{e}^{i\Delta\phi} \cos\psi + t_{\text{TE}} \sin\psi, \tag{6.4}$$

so that the signal measured by the detector can be written as:

$$S_{\text{out}} \propto t_{\text{TM}}^2 \cos^2\psi + t_{\text{TE}}^2 \sin^2\psi + t_{\text{TM}} t_{\text{TE}} \sin 2\psi \cos\Delta\phi. \tag{6.5}$$

Using the ratio $(t_{\text{TM}}/t_{\text{TE}})^2$ as measured in our transmission experiment (see Fig. 6.5) we fit the experimental data of Fig 6.6 with Eq. (6.5) taking $\Delta\phi$ as a fitting parameter. The results of a fit for the 250 nm wide slit are shown in Fig. 6.7a.

Figure 6.7b shows that the phase difference $\Delta\phi$ decreases almost linearly with increasing slit width, and so does the effective birefringence $|n_{\text{TE}} - n_{\text{TM}}|$ of the slit. The phase difference passes through a value of $\pi/2$ at $b = 250$ nm. For that slit width, however, the transmitted light is *not* circularly polarized, due to the unequal amplitudes of the TE- and TM-polarized components. Although different in the details, the results obtained with the array of slits (Figs. 6.4–6.7) fully support the initial results of Fig. 6.1. Being able to generate circularly polarized light with sub-wavelength wide slits, requires careful tuning of all slit parameters and of the incident wavelength. It is a matter of serendipity that we found those conditions in our first experiment.

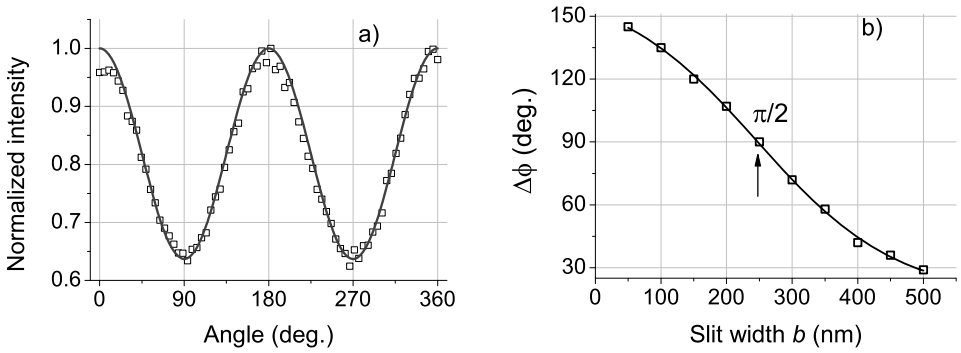

Figure 6.7. a) Example of fitting of experimental data points for the 250 nm wide slit (squares) with the model (solid line); b) Phase difference of TM and TE modes for the 200 nm deep slits as a function of slit width. The data points (squares) are obtained from a fit of the various curves of Fig. 6.6. The solid line serves to guide the eye.

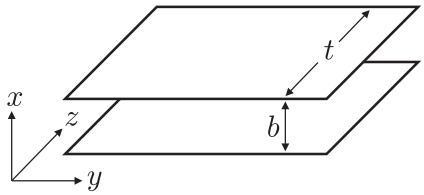

Figure 6.8. Waveguide formed by two infinitely extending plane-parallel metal sheets, separated by a distance b.

6.4 Discussion

As discussed in the introduction, the study of the transmission of electromagnetic radiation through small apertures has a long and venerable history. The standard approach to describe this, involves the study of the propagation properties of EM radiation through a waveguide with the same transverse dimensions as the slit, made from the same material as the metallic screen that carries the slit. Additionally, one has to weigh in the impedance mismatch between this waveguide and free space. Our slit forms a rectangular waveguide with a large aspect ratio (height/width). For that reason we can effectively describe each slit as a planar waveguide (see Fig. 6.8). Here we will apply such a waveguide model to see how much we can learn.

Inside the waveguide the solutions to Maxwell's equations separate into two sets of modes. For the so-called TE-modes the electric field is purely

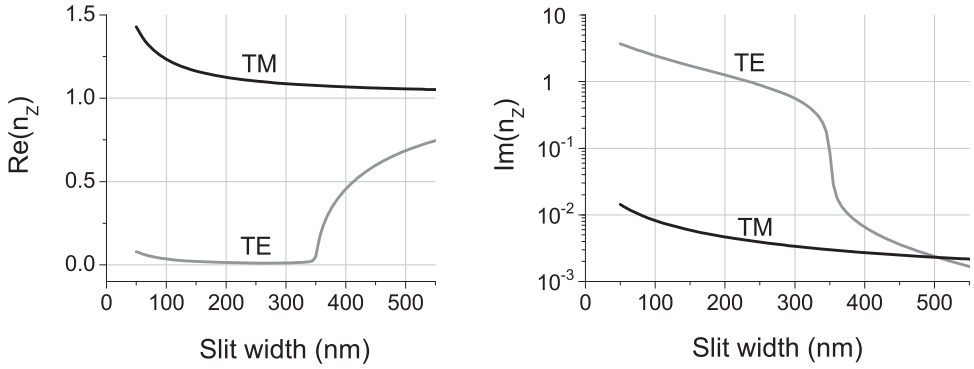

Figure 6.9. Real and imaginary parts of the mode index n_z for TM- and TE-polarized modes at $\lambda = 800$ nm in a waveguide of gold. The width of the waveguide (slit) is varied.

transverse, i.e., does not have a component in the propagation (z)-direction ($E_z = 0$); for these modes one solves the wave equation for E_y. The TM-modes have a purely transverse magnetic field and $H_z = 0$ everywhere in the waveguide; in this case one solves the wave equation for H_y.

For a monochromatic wave the dependence on space and time for E_y (TE-mode) or H_y (TM-mode) is written as:

$$\exp[i(\omega t - k_x\, x - k_z\, z)], \tag{6.6}$$

with

$$k_z = \sqrt{\frac{\omega^2}{c^2} - k_x^2}, \tag{6.7}$$

yielding

$$n_z = \sqrt{1 - \frac{k_x^2}{k_0^2}}, \tag{6.8}$$

for the mode index ($k_0 = \omega/c$). The allowed values for k_x follow from a set of matching conditions at the metallic boundaries and the requirement that, in the metal, k_x is purely imaginary [123]. These matching conditions give rise to a self-consistency equation for k_x, one for the case of a TE-wave, and one for the case of a TM-wave. The solutions of these equations for k_x are generally complex. Using Eq. (6.8) one can then determine the complex refractive indices for the TE- and TM-modes, respectively.

Figure 6.9 shows the results of such a calculation for the TE- and TM-polarized modes as a function of the slit width, at $\lambda = 800$ nm, for a waveguide

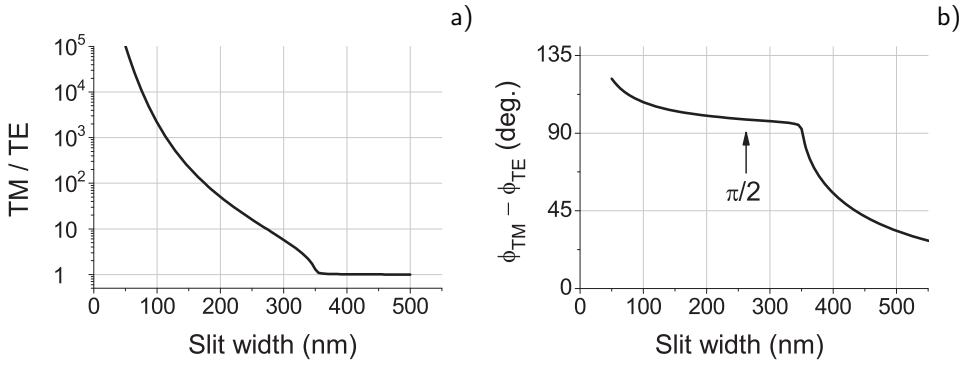

Figure 6.10. a) TM/TE transmission ratio of a 200 nm long piece of waveguide made from gold at a wavelength of 800 nm; b) Relative phase delay between the TE- and TM-modes of such a waveguide, as a function of waveguide width.

of gold. For the TM-mode both the real and imaginary parts of n_z depend weakly on the slit width b: the real part increases with decreasing slit width [41] while the imaginary part is close to zero, except at the smallest values of b, showing that the TM mode is only weakly damped. The variation of n_z is much more pronounced for the TE-mode: as b is reduced the real part of n_z drops off rapidly to becomes vanishingly small at $b \simeq 350$ nm (the cut-off width). At the same value of b the imaginary part of n_z is seen to jump by roughly a factor 50.

With the results of Fig. 6.9 we can explain most of our experimental results. First, by looking at the real part of the mode index, we see that the birefringence increases to a value of order 1, as the slit width is reduced from 500 to 350 nm. At smaller values of the slit width, the birefringence is "locked" to a value ≈ 1. From the results for the imaginary part of the mode index, we see that the dichroism explodes at $b = 350$ nm, becoming so large that the transmitted light is purely TM-polarized when the slit width is below the critical value. Actually, already at $b = 400$ nm the dichroic effect is sufficiently large that the transmitted light is predominantly TM-polarized.

From the results of Fig. 6.9 we can calculate the relative modal transmission $\exp[-4\pi\,\mathrm{Im}(n_z^{\mathrm{TM}} - n_z^{\mathrm{TE}})\,t/\lambda]$ and the relative phase delay $\Delta\phi = 2\pi t \mathrm{Re}\,(n_z^{\mathrm{TM}} - n_z^{\mathrm{TE}})$ for a section of waveguide of length $t = 200$ nm (see Fig. 6.10). It is seen that, even for such a short waveguide, the cut-off is well defined: the TM/TE transmission ratio rises rapidly for $b < 350$ nm. Moreover, we see that the TE-TM phase delay is predicted to be $\Delta\phi = \phi_{\mathrm{TM}} - \phi_{\mathrm{TE}} \approx \pi/2$ in the range $200 < b < 350$ nm, in quite good agreement with the

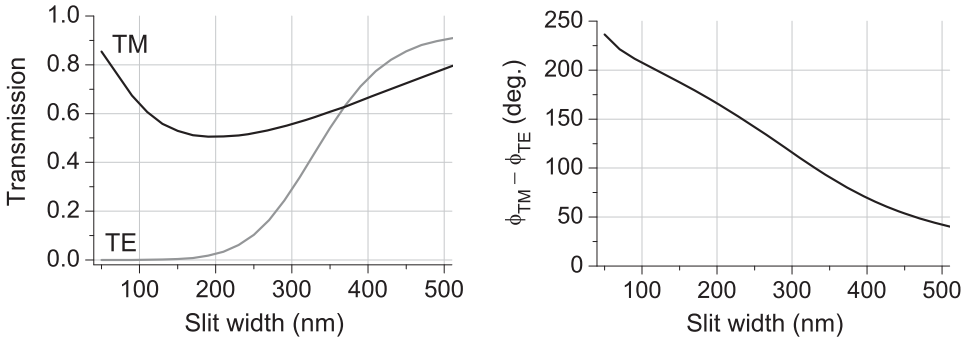

Figure 6.11. Results of a numerical calculation, based on a rigorous diffraction model, for the width-normalized transmission and relative phase delay, for a slit in a 200 nm thick gold film, studied with incident light at 800 nm.

experimental result (see Figs. 6.1 and 6.7).

Although the waveguide approach yields a reasonably prediction for the TM-TE phase slip at slit width of order 250 nm, it doesn't do such a good job in predicting the width dependence of the phase slip nor of the TM/TE transmission ratio as found in our experiments. This is not surprising since our model only accounts for the waveguide properties of the slit and does not take into account the coupling of the incident radiation with the waveguide mode, the outcoupling properties of the waveguide and the possibility of exciting surface plasmons or other surface modes.

In order to obtain a more complete picture we have turned to a rigorous diffraction model [90] where we take into account all known details of our setup. Specifically, we calculate the transmission and phase delay of a plane wave incident on the interface between a dielectric (glass) and a composite metal film consisting of 10 nm titanium metal with 200 nm gold on top. The metal sandwich is perforated by a single, infinitely long, narrow slit and the output field radiates into vacuum. We do so for both TE- and TM-polarized incident fields. The results are shown in Fig. 6.11.

Overall, the results of this calculation are in very good agreement with the experimental data of Fig. 6.4. In particular, the calculations reproduce the dip at $b \simeq 200$ nm in the transmission of the TM wave. We believe that this dip is associated with the excitation of surface plasmons. The probability of exciting these surface modes is predicted to peak when $b/\lambda \approx 1/4$ [34]. Also the gradual variation of the TE-mode transmission is well reproduced by the calculations, though the onset of transmission is shifted to larger slit

width in the calculation as compared to the experiment. The fact that for small values of the slit width the experimental TE transmission is considerably larger than predicted, can be attributed to unavoidable variations in the slit width. Small sections that have a width that is larger than the nominal value, will substantially increase the transmitted power. The calculations also do a good job in predicting the TM-TE phase difference that we have observed in the experiment yielding a $\pi/2$ phase difference between TM and TE modes at $b \simeq 350$ nm. Note, however, that the $(\phi_{\mathrm{TM}} - \phi_{\mathrm{TE}})$ curve in Fig. 6.11 is a bit steeper than that of Fig. 6.7b.

6.5 Conclusions

We have studied the transmission properties of a sub-wavelength slit milled in a 200 nm thick gold-metal film as a function of the slit width (50–500 nm), and of the polarization of the incident radiation (at $\lambda = 800$ nm). As the slit width is decreased the normalized transmission of the TE-mode diminishes quite gradually until it becomes vanishingly small at a value of the normalized slit width of order 1/8, reminiscent of the phenomenon of waveguide cut-off. In contrast, the width-normalized transmission of the TM-mode varies only by a factor of 2 when the slit width varies between 50 nm and 500 nm. In this interval it shows a characteristic dip at a slit width of order $\lambda/4$, associated with the efficient excitation of surface plasmons. Moreover, we have measured the phase slip between the TM- and TE-polarized modes through such a sub-wavelength slit. We have compared our experimental results with a simple waveguide model and with the results of a rigorous diffraction calculation. The latter shows good predictive power and is able to reproduce most of the features of our experimental results.